Optics Communications 291 (2013) 299–303

Contents lists available at SciVerse ScienceDirect

Optics Communications

journal homepage: www.elsevier.com/locate/optcom

Subexawatt few-cycle lightwave generation via multipetawatt pulse compression

Aleksandr A. Voronin [a,b], Aleksei M. Zheltikov [a,b,c,*], Todd Ditmire [d], Bedrich Rus [e], Georg Korn [e,f]

[a] Physics Department, International Laser Center, M. V. Lomonosov Moscow State University, Vorob'evy gory, Moscow 119992, Russia
[b] Russian Quantum Center, 143025 Skolkovo, Moscow Region, Russia
[c] Department of Physics and Astronomy, Texas A&M University, College Station, TX 77843-4242, USA
[d] Texas Center of High Intensity Science, University of Texas at Austin, University Station 1, Austin, TX 78712, USA
[e] Institute of Physics, Extreme Light Intensity Beamlines Facility, Prague 18040, Czech Republic
[f] Max-Planck-Institut für Quantenoptik, Hans-Kopfermann-Strasse 1, D-85748 Garching, Germany

ARTICLE INFO

Article history:
Received 24 June 2012
Accepted 17 October 2012
Available online 20 November 2012

Keywords:
Pulse compression
Extreme power lasers
Self-focusing

ABSTRACT

We identify the physical scenarios of nonlinear spatiotemporal dynamics of extreme-power laser fields enabling compression of a broad-beam ultrafast multipetawatt laser output to subexawatt few-cycle light pulses focusable to pulse intensities up to 10^{25} W/cm^2. We show that, with a careful control over the key limiting physical effects, which include dispersion, pulse self-steepening, small-scale self-focusing, and ionization effects, enhanced self-phase modulation of multipetawatt laser waveforms in a solid medium can provide spectral bandwidths compressible to few-cycle pulse widths with output beam profiles focusable to ultrarelativistic intensities.

Following 50 years of discoveries and groundbreaking technological achievements, the laser science is on the verge of breaking through to the exawatt peak power level [1]. With petawatt to multi-petawatt laser technologies coming of age [2–5], progressing toward higher efficiencies, repetition rates, beam quality, and reliability, one promising strategy for the creation of exawatt lasers is based on coherent combining of petawatt laser beams [1]. In this paper, we demonstrate an alternative approach to reach peak powers nearing an exawatt level employing pulse compression of multipetawatt laser pulses. We examine the possibility of generating additional bandwidth with a multi-petawatt laser pulse through self-phase modulation in a nonlinear medium and calculate how this additional bandwidth could be compressed to yield exawatt-class peak powers. Such multipetawatt lasers will soon be available. Through the physical scenarios described here, the output of these lasers could be compressed to few-cycle field waveforms. The key physical effect enabling this pulse-compression strategy is self-phase modulation of multipetawatt laser pulses due to the Kerr nonlinearity of a solid-state medium. The main limiting processes, intrinsically built into the strongly coupled spatial and temporal nonlinear-optical transformations of extreme-power laser fields, include dispersion, pulse self-steepening, small-scale self-focusing, and ionization. Our analysis presented below demonstrates that, with a careful control over these limiting physical effects, self-phase modulation of multipetawatt laser waveforms in a solid medium can be enhanced to generate spectral bandwidths compressible to few-cycle pulse widths with output beam profiles focusable to ultrarelativistic intensities. Unlike power boosting schemes based on laser or parametric amplification, nonlinear-optical phenomena can help raise the peak power of laser pulses without an external energy supply. The spectral broadening of laser pulses induced by nonlinear-optical interactions is free of limitations imposed by a finite gain band of a laser or parametric amplifier, enabling compression to pulse widths as short as a fraction of a field cycle [1,2].

Identifying the physical scenarios that would enable efficient spectral transformation of extreme-power laser pulses in nonlinear media is a challenging problem, which involves several fundamental issues of extreme-light–matter interactions. In particular, as shown by Bespalov and Talanov more than four decades ago [6], along with self-focusing of a beam as a whole, high-power laser light can exhibit small-scale self-focusing due to the spatial modulation instability of the beam relative to small intensity variations across the laser beam and small spatial inhomogeneities in the optical properties of nonlinear media. The spatiotemporal dynamics of ultrahigh-power laser beams gives rise to multifilamentary structure of the field, which has been verified by numerous laser experiments in gases, liquids, and solids (see Refs. [7,8]for a review). Within a limited range of parameters, the breakup of a laser beam into multiple filaments can be suppressed with the use of specifically designed spatial

* Corresponding author at: Physics Department, International Laser Center, M. V. Lomonosov Moscow State University, Vorob'evy gory, Moscow 119992, Russia. Tel.: +7 495 9395174; fax: +7 495 939 3113.
E-mail addresses: zheltikov@physics.msu.ru, zheltikov@physics.tamu.edu (A.M. Zheltikov).

0030-4018/$ - see front matter © 2012 Elsevier B.V. All rights reserved.
http://dx.doi.org/10.1016/j.optcom.2012.10.057

filters [9,10]. Ultrafast laser-induced ionization at the hot spots, arising across the laser beam during the initial phase of multiple filamentation, results in irreversible modifications and, eventually, a damage of the nonlinear material. Because of the stochastic nature of laser intensity fluctuations across the laser beam and a very fast, femto- to atto-second time scale of laser-induced ionization processes [11,12], ionization-related effects in the field of ultrashort laser pulses are extremely difficult to regularize, which drastically complicates the design of practical optical devices implementing this strategy of pulse transformation.

In this work, we address these issues by performing a detailed analysis of the spatiotemporal dynamics of high-power laser pulses in a nonlinear, fast-ionizing solid-state medium in a pulse transformation scheme sketched in Fig. 1(a). Our analysis is based on the numerical solution of the three-dimensional time-dependent generalized nonlinear Schrödinger equation [7,8,13,14] for the amplitude of the laser field propagating through a nonlinear medium. This model includes the key physical effects in the evolution of ultrashort light pulses, such as dispersion of the medium, beam diffraction, Kerr and Raman optical nonlinearities, pulse self-steepening, spatial self-action phenomena (including self-focusing of a beam as a whole and small-scale self-focusing), ionization-induced optical nonlinearities, as well as plasma loss and dispersion. The field evolution equation is solved jointly with the rate equation for the electron density, which includes photoionization [15] and impact ionization. Typical parameters of fused silica [7,8] have been used in simulations, including the band gap $U_i \approx 9$ eV, the nonlinear refractive index $n_2 \approx 3 \times 10^{-16}$ cm^2/W, a damped oscillator model of the Raman response, and the collision time in the Drude-model impact ionization cross section $\tau_c \approx 1.7$ fs. The input field is assumed to have a Gaussian temporal pulse shape, a super-Gaussian spatial beam profile (Fig. 1(a)), a peak power of 13 PW, a pulse width of 120 fs, and a beam diameter of 40 cm. This set of parameters mimics the output of multi-petawatt laser systems planned for the near future [5].

Simulations were performed in parallel codes on the Lomonosov supercomputer of Moscow State University using a split-step Fourier method, with the nonlinear part solved by the implicit fifth-order Runge–Kutta method. We used a variable step along the z-axis, which has been adjusted in such a way as to keep the nonlinear phase shift of the laser field at each step below 0.1 rad. Discretization steps in time and transverse coordinates x and y in these simulations (0.27 fs and 1 μm, respectively) were chosen in such a way as to provide a reliable convergence of the numerical procedure.

To model multiple filamentation of high-power laser pulses in the nonlinear medium, we seed spatial modulation instabilities by superimposing a Gaussian-noise modulation with a standard deviation of 0.0185 on the input beam profile (Fig. 1(b)). Self-phase modulation due to the Kerr-type optical nonlinearity of silica is seen to lead to an efficient spectral broadening (Fig. 2(a)), with the asymmetry of the output spectra caused by the self-steepening of laser pulses. As the laser pulse propagates through the nonlinear medium, small-scale self-focusing of the laser beam amplifies the input noise on the laser beam, giving rise to hot spots in the beam profile (Figs. 1c, 3a). Enhanced free-carrier generation at these hot spots (Fig. 3(b)) increases the risk of laser damage. These processes, along with the dispersion of the solid-state medium, eventually limit the maximum propagation length and, hence, the maximum bandwidth of the output pulse.

To identify the physical factors controlling the observed spatiotemporal dynamics of the laser field, we compare the results

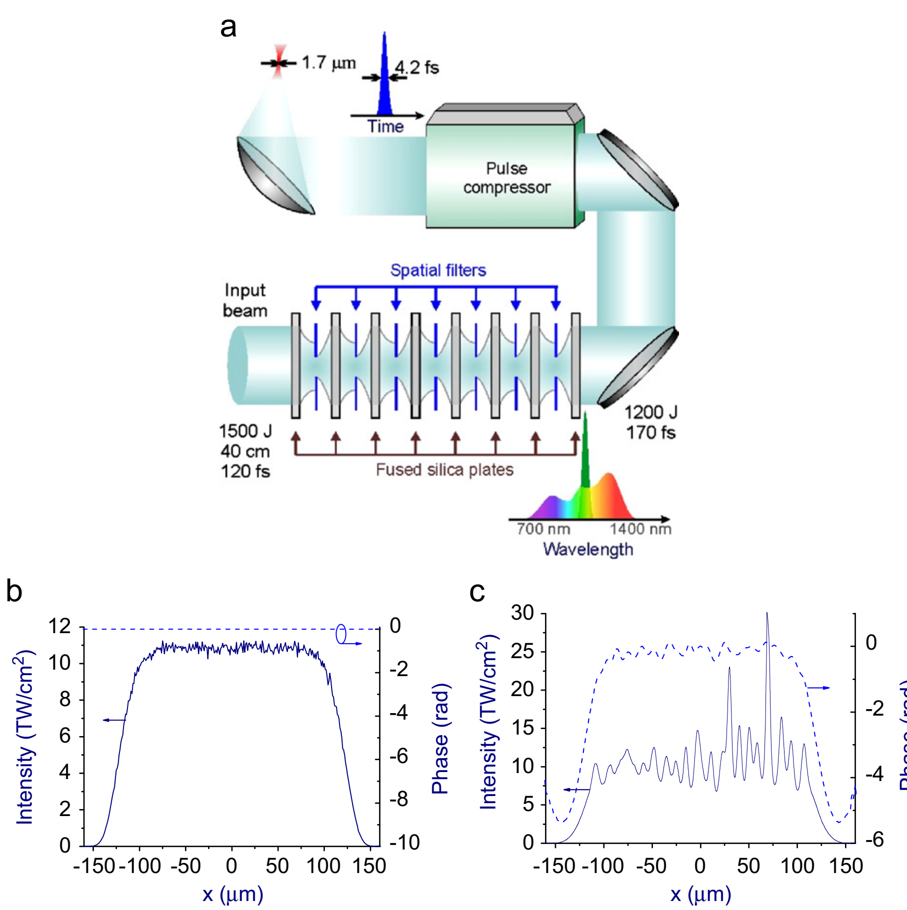

Fig. 1. (a) Compression of a multipetawatt laser pulse. (b, c) Transverse intensity (solid line) and phase (dashed line) profiles in the laser beam: (b) the input beam with a Gaussian noise with a standard deviation of 0.0185 and (c) the beam transmitted through a 270 μm-thick silica plate.

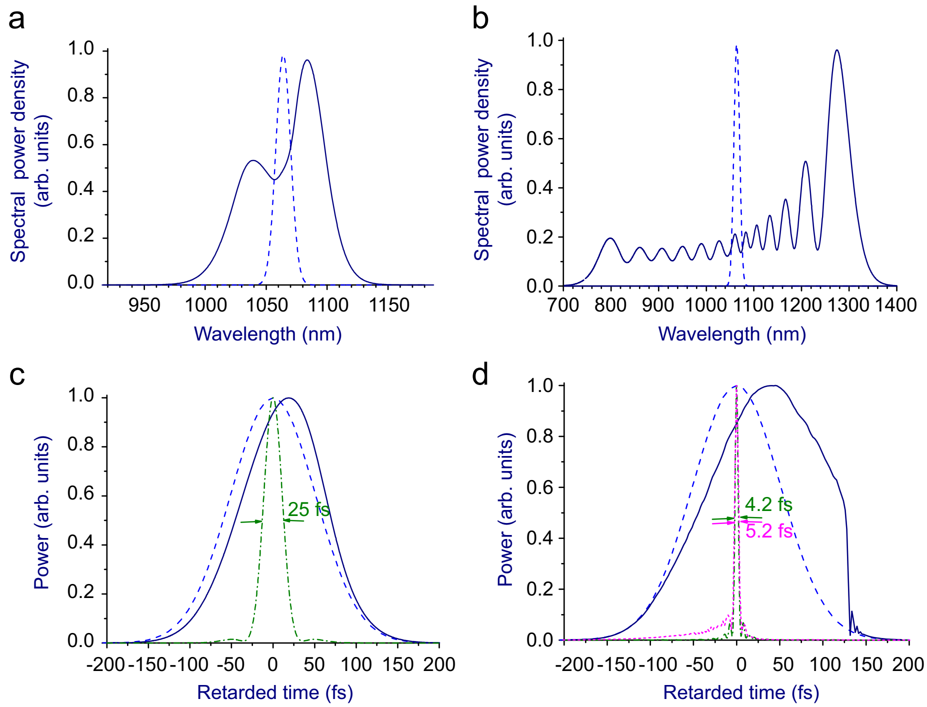

Fig. 2. The spectra (a, b) and temporal profiles (c, d) of the input laser pulse (dashed line) and the laser pulse transmitted (a, c) through a 270-μm-thick silica plate (solid line) and (b, d) through a cascade of nine nonlinear elements separated by eight spatial filters (sketched in Fig. 1a). The envelopes of the spectrally broadened pulses compressed to their transform limit (dash-dotted lines in panels c, d) and the pulse envelope following linear chirp compensation (dotted line in panel d).

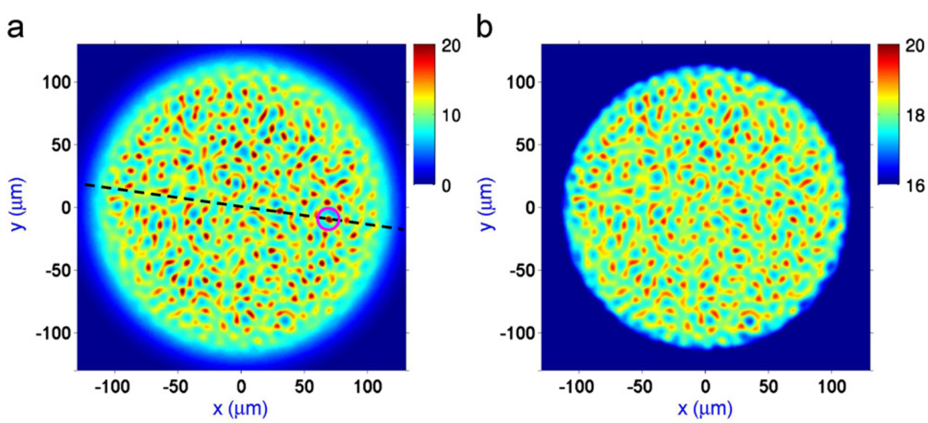

Fig. 3. Field intensity (a) and electron-density (b) profiles within the laser beam with a Gaussian noise with a standard deviation of 0.0185 transmitted through a 270 μm-thick silica plate. A small fragment of a laser pulse is shown for a better visibility of hot spots. The field intensity profile in Fig. 1(c) is along the direction shown by the dashed line in panel (a). Encircled is the hotspot of maximum intensity (30 TW/cm^2).

of numerical simulations with the analytical predictions of the Bespalov–Talanov theory of small-scale self-focusing [6]. According to this theory, a steady-state wave $E_0 = B_0 \exp(-i\Phi)$, with $\Phi = \omega n_2 (2c)^{-1} |B_0|^2 z$, is unstable with respect to a small harmonic perturbation $E_1 = B_1(z)\cos(2\pi q r)\exp(-i\Phi)$, where $r = (x^2+y^2)^{1/2}$ and q is the transverse wave number. The maximum value of modulation instability gain $K(q) = |B_1(z)|/|B_0|$ is achieved [6,16] for perturbations with the phase:

$$\phi_{\max} = -\frac{3\pi}{4} - \frac{1}{2}\arctan\left[\frac{Q-\Phi}{\kappa Q}\tanh(\kappa Q)\right] + \pi m \quad (1)$$

and is given by

$$K_{\max} = \frac{\Phi}{\kappa Q}\sin h(\kappa Q) + \left\{1 + \left[\frac{\Phi}{\kappa Q}\sin h(\kappa Q)\right]^2\right\}^{1/2} \quad (2)$$

where $\kappa = 2\pi^2 q^2 c (n_0\omega)^{-1} z$, $Q = (2\Phi\kappa^{-1} - 1)^{1/2}$, and m is an integer.

The dashed line in the inset of Fig. 4(a) shows the instability gain calculated using Eq. (1) for laser pulses with the above-specified parameters transmitted through a 270 μm silica plate. The maximum modulation instability gain is achieved for spatial inhomogeneities with a size $d \approx (\pi P_{cr}/I_0)^{1/2}$, where P_{cr} is the critical power of self-focusing and I_0 is the peak intensity. With $P_{cr} \approx 3$ MW (for silica at a wavelength of 1 μm) and $I_0 \approx 10$ TW/cm^2 (for the chosen parameters of laser pulses), we find $d \approx 10$ μm. The solid line in the inset of Fig. 4(a) presents the simulated spatial spectrum of a laser pulse with the above-specified parameters after propagating through a 270 μm silica plate. This spectrum is normalized to the angular spectrum of the input field and to the spatial spectrum of the input field. Although the Bespalov–Talanov theory is, rigorously speaking, applicable only for harmonic perturbations of continuous-wave fields, this theory provides an adequate approximation for the spatial spectrum of modulation instability gain of a high-power laser beam in a nonlinear medium, as well as for the typical spatial scale

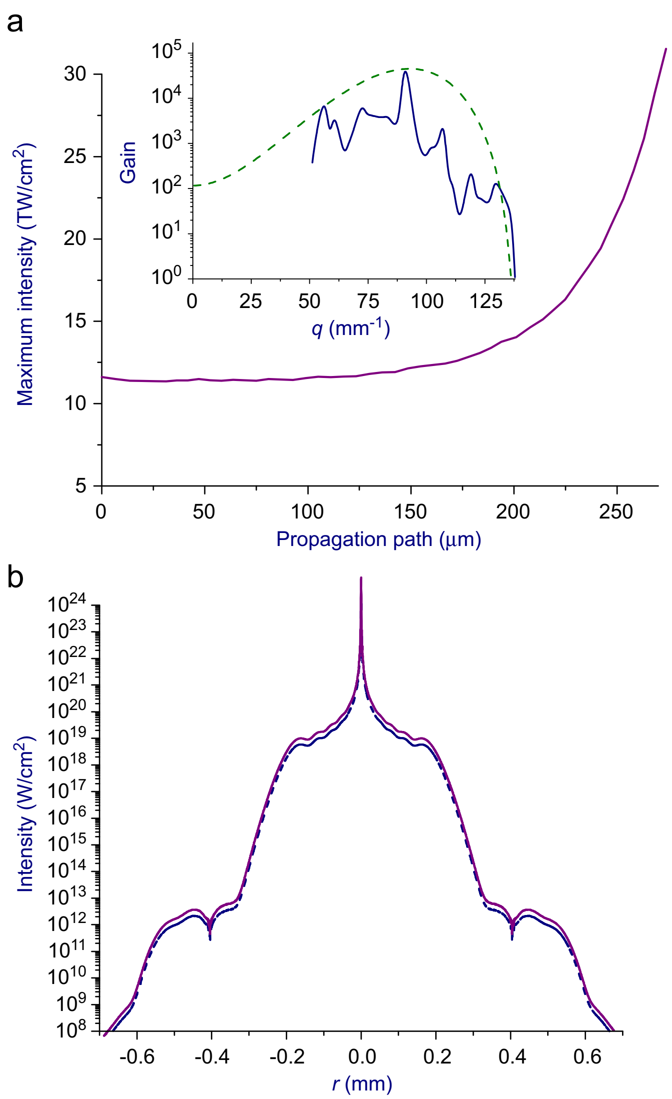

Fig. 4. (a) The maximum field intensity $I_m(z)$ at hotspots within the laser beam as a function of the propagation length in a nonlinear medium. The inset shows the numerically simulated spatial spectrum of a laser pulse transmitted through a 270 μm silica plate normalized to the angular spectrum of the input field (solid line) and the spectrum of modulation instability gain calculated with the use of Eq. (2) for a laser beam with the same parameters (dashed line). (b) The spatial profile of field intensity in the compressed laser pulse focused with a 40 cm-diameter, 40 cm-focal-length mirror for a pulse where only the linear chirp is compensated (dashed line) and where both quadratic and cubic phases are compensated (solid line).

of the filamentary structure that tends to show up in the beam profile. This point is illustrated in Fig. 4(a). Both numerical simulations and Eq. (2) yield modulation instability gain spectra featuring a cutoff around $q_{\max} \approx 100$–$120\ \mathrm{mm}^{-1}$, corresponding to transverse inhomogeneities of the beam profile with a typical size of $d \approx 1/q_{max} \approx 8$–$10\ \mu\mathrm{m}$. This estimate agrees very well with the sizes of the hot spots observed in the beam profile in Fig. 3(a). Spatial inhomogeneities of smaller sizes do not evolve into a filamentary structure of the beam, because their transverse wave numbers fall beyond the cutoff of the modulation instability gain spectrum.

To illustrate limitations on the propagation length in a nonlinear medium imposed by the small-scale self-focusing dynamics of a high-power laser beam, we compute transverse field intensity profiles $I_0(x, y, z)$ at the peak of the pulse for different propagation lengths and define the maximum field intensity $I_m(z) = \max_{x,y} \{I_0(x,y,z)\}$ over the entire beam for each z. The $I_m(z)$ dependence, presented in Fig. 4(a), shows that the field intensity at the hot spots exhibits a rapid growth, which, in the case of a single discontinuous slab of nonlinear material, becomes especially dramatic for $z > 270\ \mu\mathrm{m}$. Computing transverse electron density profiles in the wake of the laser pulse for different z and defining the maximum electron density $\rho_m(z) = \max_{x,y}\{\rho_0(x,y,z)\}$ over the entire beam for each z, we find that the electron density of $0.1\rho_c$ (where ρ_c is the critical plasma density), which is often taken as a fuzzily defined criterion of optical damage [7,8,17], is achieved around $z \approx 280\ \mu\mathrm{m}$. For the chosen parameters of laser pulses, the propagation length thus needs to be restricted to $z < 270\ \mu\mathrm{m}$.

If the laser intensity in the hotspots is kept below the laser damage threshold, a bandwidth supporting pulse compression to ~25 fs pulse widths (Fig. 2(c)) can be generated using a 270 μm silica plate. This yields a compressed pulse with a peak power of about 60 PW. While the pulse shown in Fig. 2(c) is obtained with an assumption of ideal pulse compression to the transform-limited pulse width, simple linear chirp compensation gives a very close result, since the nonlinear phase shift in the considered regime is dominated by self-phase modulation. A compensation of small third-order phase distortions with a chirped-mirror compressor [18] yields a pulse almost identical to the transform-limited pulse in Fig. 2(c).

The peak power of compressed pulses can be further increased through the use of spatial filters, consisting of $f/10$ focusing mirrors and 4.3 mm-diameter diaphragms placed in the focal planes of these mirrors. The hotspots in the spatial profile of the beam behind each silica plate give rise to a background on the periphery of the focused beam. This background is filtered out by the respective diaphragm. The improved-quality beam is then collimated with an $f/10$ mirror and transmitted through the next silica plate (Fig. 1(a)). Diameters of the diaphragms were chosen in such a way as to keep the laser intensity on diaphragm orifices below the laser damage threshold. The maximum laser fluence on the mirrors, on the other hand, was kept below 3 J/cm^2 to avoid the laser damage of mirrors. With spatial filters, the laser pulses can be transmitted through a much larger length in a nonlinear material without a catastrophic degradation of beam quality. In Fig. 2(b), we present the spectrum of a laser pulse with the same input parameters as above transmitted through a cascade of nine silica plates separated by eight spatial filters, yielding a total nonlinear interaction length of 2.43 mm. The output bandwidth of this pulse supports temporal compression to a transform-limited pulse width of 4.2 fs (the dash-dotted line in Fig. 2(d)). When only the linear chirp is compensated, the pulse is compressed to a pulse width of 5.2 fs (the dotted line in Fig. 2(d)), leading to a peak power in excess of 350 PW. The overall energy loss due to the spatial filtering in the considered system is 15%. A further increase in the number of silica plates does not lead to a more efficient pulse compression because of pulse self-steepening, which is readily seen in the temporal profile of the laser pulse shown by the solid line in Fig. 2(d).

Focusing such a compressed pulse with a 40 cm-diameter, 40 cm-focal-length mirror yields a beam profile shown in Fig. 4(b). The maximum intensity attainable with this focusing geometry is $6 \cdot 10^{24}$ W/cm^2 for a pulse where only the linear chirp has been compensated (the dashed line in Fig. 4(b)) and approximately 10^{25} W/cm^2 for a pulse following both quadratic and cubic phase compensation (the solid line in Fig. 4(b)). Two types of beam distortions are identified for the focused laser beam in Fig. 4(b). The higher-level background, observed for $|r| \leq 0.3$ mm in Fig. 4(b) is due to the self-focusing of the beam as a whole in the nonlinear elements. The lower-amplitude background, on the other hand, stems from the small-scale self-focusing (hotspots). As can be seen from these plots, a careful optimization of the pulse compression regime can help minimize beam-profile distortions of the compressed pulse induced by spatial self-action effects, providing a contrast of the peak intensity in the focused beam relative to the background on the periphery of the beam in excess of 10^5.

In conclusion, we have identified the physical scenarios of nonlinear spatiotemporal dynamics of extreme-power laser fields allowing a broad-beam ultrafast multipetawatt laser output to be compressed to subexawatt few-cycle light pulses. We have shown that, with a careful control over the limiting physical effects, including dispersion, pulse self-steepening, small-scale self-focusing, and ionization, self-phase modulation of multipetawatt laser waveforms in a solid medium can be enhanced to generate spectral bandwidths compressible to few-cycle pulse widths with output beam profiles focusable to ultrarelativistic intensities. The proposed scheme can be scaled to higher peak powers by increasing the beam area at a constant field intensity. The regime of nonlinear-optical transformation of multipetawatt laser pulses considered in this paper offers an attractive strategy for the generation of subexawatt few-cycle light waveforms with ultrarelativistic peak intensities in a focused beam.

Acknowledgment

Valuable help of A.V. Mitrofanov is gratefully acknowledged. This work was supported in part by the Russian Foundation for Basic Research, Welch Foundation (grant no. A-1801), and Skolkovo Foundation (grant no. 78).

References

[1] G. Korn, P. Antici (Eds.), Extreme Light Infrastructure: Grand Challenges, Paris, 2009; G. Mourou,G. Korn, W.. Sandner , J. Collier (Eds.), ELI—Extreme Light Infrastructure (Whitebook), CNRS, Paris 2011.
[2] M.D. Perry, G. Mourou, Science 264 (1994) 917.
[3] M.D. Perry, D. Pennington, B.C. Stuart, G. Tietbohl, J.A. Britten, C. Brown, S. Herman, B. Golick, M. Kartz, J. Miller, H.T. Powell, M. Vergino, V. Yanovsky, Optics Letters 24 (1999) 160.
[4] Y. Kitagawa, H. Fujita, R. Kodama, H. Yoshida, S. Matsuo, T. Jitsuno, T. Kawasaki, H. Kitamura, T. Kanabe, S. Sakabe, K. Shigemori, N. Miyanaga, Y. Izawa, IEEE Journal of Quantum Electronics 40 (2004) 281.
[5] E.W. Gaul, M. Martinez, J. Blakeney, A. Jochmann, M. Ringuette, D. Hammond, T. Borger, R. Escamilla, S. Douglas, W. Henderson, G. Dyer, A. Erlandson, R. Cross, J. Caird, C. Ebbers, T. Ditmire, Applied Optics 49 (2010) 1676.
[6] V.I. Bespalov, V.I. Talanov, JETP Letters 3 (1966) 307.
[7] L. Bergé, S. Skupin, R. Nuter, J. Kasparian, J.-P. Wolf, Reports on Progress in Physics 70 (2007) 1633.
[8] A. Couairon, A. Mysyrowicz, Physics Reports 441 (2007) 47.
[9] A.K. Potemkin, E.A. Khazanov, M.A. Martyanov, M.S. Kochetkova, IEEE Journal of Quantum Electronics 45 (2009) 336.
[10] J.T. Hunt, J.A. Glaze, W.W. Simmons, P.A. Renard, Applied Optics 17 (1978) 2053.
[11] A.J. Verhoef, A.V. Mitrofanov, E.E. Serebryannikov, D.V. Kartashov, A.M. Zheltikov, A. Baltuška, Physical Review Letters 104 (2010) 163904.
[12] A.V. Mitrofanov, A.J. Verhoef, E.E. Serebryannikov, J. Lumeau, L. Glebov, A.M. Zheltikov, A. Baltuška, Physical Review Letters 106 (2011) 147401.
[13] M. Geissler, G. Tempea, A. Scrinzi, M. Schnürer, F. Krausz, T. Brabec, Physical Review Letters 83 (1999) 2930.
[14] A.M. Zheltikov, A.A. Voronin, R. Kienberger, F. Krausz, G. Korn, Physical Review Letters 105 (2010) 103901.
[15] L.V. Keldysh, Zh. Eksp, Teor. Fiz, Soviet Physics—JETP 47 (1964) 1945; L.V. Keldysh, Soviet Physics—JETP 20 (1965) 1307.
[16] S.G. Garanin, I.V. Epatko, R.V. L.V. L'vov, Serov, S.A. Sukharev, Quantum Electronics 37 (2007) 1159.
[17] A. Couairon, L. Sudrie, M. Franco, B. Prade, A. Mysyrowicz, Physical Review B 71 (2005) 125435.
[18] V. Pervak, I. Ahmad, S.A. Trushin, Zs. Major, A. Apolonski, S. Karsch, F. Krausz, Optics Express 17 (2009) 19204.